STUDIES ON BUCKLING AND FAILURE OF PROJECTILES UNDER PERFORATION

X.W. Chen[1], Y.B. He, G. Chen and M. Qu

Institute of Structural Mechanics, China Academy of Engineering Physics,
P.O. Box 919-414, Mianyang City, Sichuan Province, 621900, China
[1]corresponding author. E-mail: chenxiaoweintu@yahoo.com

Different projectiles may undergo much severe failure and damage under high velocity impacts, e.g. in the case of deep penetration into High Strength Concrete (HSC) and super-sonic perforation into steel plate. The paper presents the experimental and numerical studies on buckling and failure of projectiles under different impacts. The first scenario is the transition of three failure modes of Fragment Simulation Projectiles (FSP), i.e., Taylor impact, Petal-cap failure of Sunflower alike and Plugging perforation which observed in tests of A3 steel blunt projectiles impacting 45 steel plates. The second scenario is the dynamic plastic buckling of thin-wall projectiles. Two failure modes, i.e., axial crapy inflation and axial evaginable tearing for different length-diameter-ratio projectiles, are observed in test. Numerical simulations are conducted to display the failure and damage process of projectiles. It confirms these failure modes in different scenarios and agrees well with the experimental phenomena.

INTRODUCTION

Theoretical analysis, experimental study and numerical simulation are the parallel research methods in the penetration mechanics. In general, some reasonable estimation and approximate prediction can be conducted based on the theoretical analysis, in which some assumptions and modelling predigestions are usually employed. In site test of penetration is always expensive, and only very limited test result can be obtained due to the restricted experimental condition accompanied with loss of the majority of process data. Numerical simulation may repeat the main results of in site test and offer a large amount of process information, while it only needs very lower cost, and usually we call it as the numerical test. Structural design and analysis of warhead relies on the numerical test more and more than anytime before. The paper presents our attempts to combine the theoretical analysis, experimental study and numerical simulation on the failure and rapture of projectiles under penetration and perforation.

EXPERIMENTAL OBSERVATIONS ON THREE FAILURE MODES OF FSP

One of the backgrounds of weaker projectile striking harder metal plate is the terminal ballistics of fragment warheads. Yaziv, et. al. [1] reported an experimental study of fragment simulated projectile (FSP) impacting onto steel plates, and observed two modes of penetration mechanisms, i.e., it transforming from Taylor impact to plate plugging under adiabatic shear failure.

The present paper [2,3] conducted an experimental study of A3(Q235A) steel blunt projectiles striking at 45 (1045 in US) steel plates under velocity varying from 200m/s to 800m/s. A3 steel is weaker than 45 steel. Similarly, Taylor impact and plate plugging are observed in the velocity ranges of 200m/s-400m/s and 700m/s-800m/s, respectively. However, in the velocity range of 400m/s-700m/s, a new failure mode of projectile, i.e., petal-cap failure of Sunflower alike, is further observed. Fig. 1 includes almost all the residual projectiles after impact, and clearly indicates the transition of three failure modes of projectiles under different impact velocities.

Different from ideal Taylor impact, the deformations of projectiles evolve from continual plastic flow to local petal cracks. In general, the mushroom bottom includes two parts of inner and outer loops, and the petal cracks always stop at the interface of inner and out loops. With increasing the impact velocity, the petal cracks may develop and separates from the inner loop and further forms as Sunflower petals.

Different Sunflowers change from blooming to fructiferous, and then to wizen. As shown in Fig. 2, the protruding spherical caps gradually become bigger and higher. Concomitantly, petals pullulate and enlarge so that they become evaginated and inflected. Furthermore, spherical protruding cap may completely break away from projectile. Streamlines of fountain-conflux type appear in the surface of renegade cap.

Plugging perforation dominates in the whole impact process of higher velocity. With comparing to the prototypes, all the residual projectiles lose a large amount of mass and shorten the lengths. The heads of projectiles obviously become blunter and look like a mushroom cylinder with a smooth spherical cap.

Figure 1. Variations of failure modes of projectiles under various impacts

Figure 2. Petal-cap failure of Sunflower alike

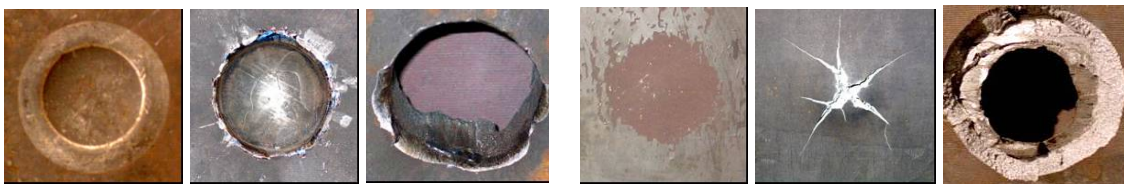

Figure 3. Typical failures of front and rear surfaces of target plates under three impact modes

Typical failures of front and back faces of steel plates are given in Fig.3. Inner and outer loops can be identified in the shallow indentation of Taylor impact, and only a little bulge occurs in the back face of target. In the case of mode II, front crater becomes deeper and even reach the bottom of plate. In the case of mode III, shear plugging and brittle fracture are observed in the front and rear sections of bullet hole, respectively.

NUMERICAL SIMULATIONS ON THREE FAILURE MODES OF FSP

LS-DYNA3D is employed to simulate FSP failure [4]. Johnson-Cook models of strength and accumulative damage failure are employed to characterize the material behaviours of projectile and target with accounting for adiabatic temperature rise.

Mode I: Taylor Impact

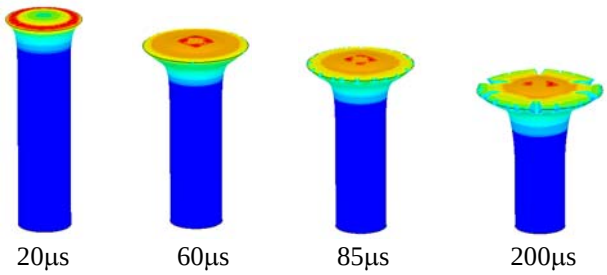

Figure 4. Deformation process of Taylor impact of projectile

Fig.4 shows the projectile deformation of Taylor impact at velocity of 350m/s. Petal cracks initiate in the outer loop of mushroom and stop at the interface of inner and outer loops. Accompanied with the continuance of impact, the length of projectile becomes shorter whilst mushroom increases. The mushroom of projectile begins to initiate cracks at about 60 μs. Subsequently, some initiated cracks undergo evolutional development to create large cracks while the other cracks are restrained.

Mode II: Petal-Cap Failure of Sunflower Alike

Fig.5 shows the petal-cap failure of Sunflower alike of projectile impacting at velocity of 550m/s. Accompanied with occurrence of the protruding cap of projectile and the concave crater of target, the impact head of projectile begins to mushroom. With enlarging the outer loop of mushroom, petal cracks may arise and develop since its hoop stress overcomes its strength, and stop at the interface of inner and outer loops. Petals pullulate and further enlarge so that they become evaginated and inflected.

As shown in Fig. 6, the numerical simulation seems same as the experimental observation in Fig. 2. That means, the higher the impact velocity, the more evident mushrooming of projectile. With increasing the impact velocity, different sunflowers change from blooming to fructiferous, and then to wizen. Under higher velocity impact (exactly with higher kinetic energy), petals may fracture and breakaway from projectile when projectile begins to rebound up in the subsequent structural response.

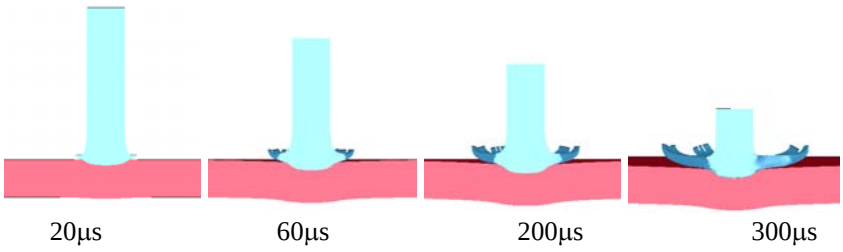

Figure 5. Deformation process of petal-cap failure of Sunflower alike (550m/s)

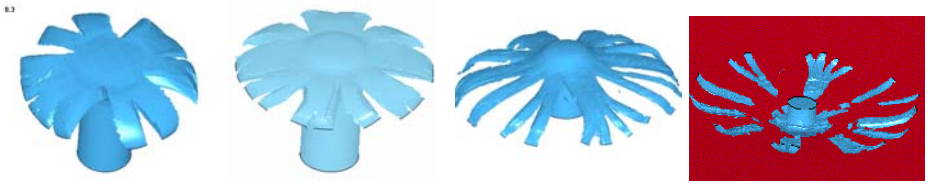

Figure 6. Different status of sunflowers under different impact conditions

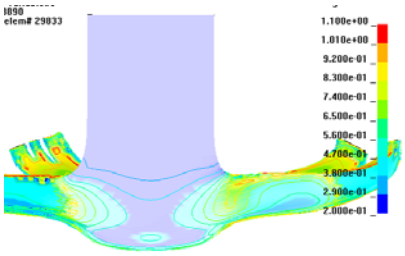

Figure 7. Contour distribution of damage of projectile (550m/s)

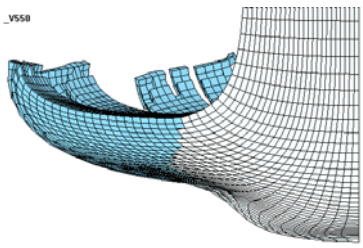

Figure 8. Mesh distortion of projectile

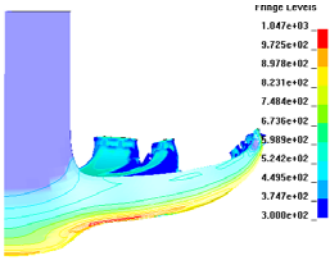

Figure 9. Adiabatic temperature rise induced by local plastic deformation

Fig. 7 shows the contour distribution of damage parameter of projectile impacting target at velocity of 550m/s. Similar to the experimental observation, in the head of the protruding cap of projectile, i.e., the stationary/death zone (inner loop) of the mushroom, the damage parameter is quite smaller. Further evolution of this zone leads to the separation of spherical protruding cap from projectile. The mesh distortion of projectile in Fig. 8 clearly displays the plastic flow of projectile material around the stationary/death zone of mushroom. Fig. 9 shows the largest adiabatic temperature rise induced by local plastic deformation may exceed 1000K.

Model III: Plugging Perforation

Fig. 10 shows the simulation of plugging perforation at velocity of 750m/s. In the initial impact stage, concave crater arises in the front face of target plate similar to the mode II. Subsequently, the depth of crater increases, and projectile head obviously become blunter as a mushroom. Like a hemispherical projectile impacting plate, all the petals are scuttled and crashed from the projectile due to the obstruction from target plate. Cracks initiate in the rear face of target and develop backward to the impact face. The projectile drills through the target plate with a plug. It further indicates that the plugging perforation is a subsequent result of continuous perforation of projectile after petal-cap failure of Sunflower alike under higher velocity impact.

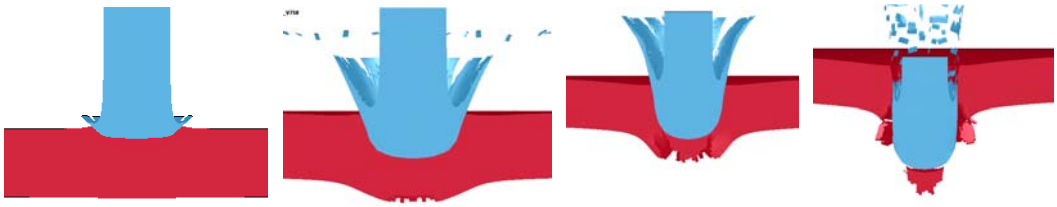

Fig.10 Simulation of the perforation of the plate struck by the projectile (750m/s)

EXPERIMENTAL OBSERVATIONS ON BUCKLING OF PROJECTILES

The intensive load may lead to severely structural destruction when a slender thin-wall projectile impacting into steel plate or high-strength concrete at high speed [5]. Besides the well known compressive/tensile failure and bending failure of missile structure, a third failure mode, i.e., dynamic plastic buckling of thin-wall projectile may induce instability of structural rigidity, and thus results in the destruction of projectile.

Fig. 11 shows all the residual projectiles after impacting 45 steel plates at different velocities [6]. Totally six projectiles are fired, with CRH=3 and different length-diameter-ratio (L/d =6, 8, 10) and wall thicknesses (h_t/d=0.10, 0.15), where L, d=25mm and h_t are the length, diameter and wall thickness of projectile, respectively. Projectile material is D6A steel and is filled with macromolecule composite. Obviously, it behaves as dynamic plastic buckling and rupture of thin-wall structure. Each projectile destructs and especially the forepart segment of shell almost crashes. Two modes of buckling failure, i.e., local axial crapy inflation and axial evaginable tearing, are observed in the middle and aft segments of shell for different length-diameter-ratio projectiles.

Regarding to the shorter projectiles (L/d=6), the destruction of projectile behaves as dynamic plastic buckling of axial crapy kind. Obvious a blunter drum is observed in projectile II-4. With comparing to II-4, projectile I-4 has much distinct damage because of thinner wall and higher impact velocity. Failure of projectile shell seems as hoop fracture and the broken strips even may scrabble up. The sharp projectile deforms severely to blunter nose and perforates the target plate as shear plugging.

Regarding to the longer projectiles of types III, IV, V and VI (L/d=8 and 10), the failure of middle and aft segments of projectile shells behaves as axial evaginable tearing with larger residual axial strips. Under impacts of similar velocities, the weaker the structural rigidity, the more notable the destruction of projectile. Comparatively, projectiles III-4 and V-4 with h_t/d=0.10 destruct severely rather than IV-4 and VI-4 with h_t/d=0.15. The impact velocity of VI-4 is the smallest, and its aft segments almost keep integrity while the middle segment obviously inflates after impact.

Figure 11. Broken projectiles after penetration tests under different velocities

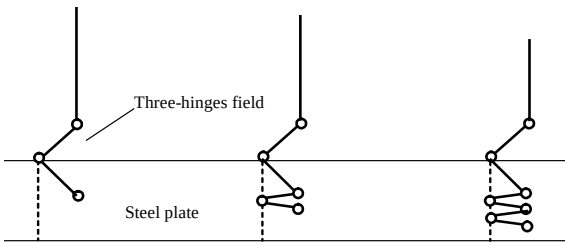

Figure 12. kinetic field of axial crapy buckling

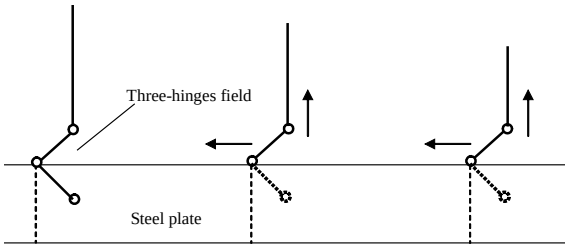

Figure 13. kinetic field of axial evaginable tearing

Fig. 12 and Fig. 13 indicate the kinetic fields of two modes of buckling failure, respectively. Three hinges distribution may be employed to describe the initial stage of buckling. However, the different subsequent development of hinge distribution due to the different surround constraining conditions leads to two kinds of buckling failure.

NUMERICAL SIMULATIONS ON BUCKLING OF PROJECTILES

LS-DYNA3D is also employed to simulate the dynamic plastic buckling of thin-wall projectiles [7]. The mutual action of projectiles and targets in Fig. 14 shows the two typical buckling failures, respectively. Basically, the initial stages of buckling of different thin-wall projectiles are very alike, i.e., all the buckling initiates at the shoulder of projectile (or the connection position of nose and cylindrical shell) after the projectile nose immerses into target partly or totally. It inflates annularly at very high speed and finally forms as annular distribution of three plastic hinges. The axial carrying capacity of thin-wall projectile decreases sharply and it induces the structural weakening. Subsequently, instable fracture occurs in the exterior edge of annular inflation and thus the backfill overflows. The numerical simulation indicates that, the configuration of buckling is dependent of the geometry of projectile, initial impact conditions and target materials.

Projectiles I and II have stronger structural rigidity because of smaller length-diameter-ratio. At the initial stage of buckling, higher impact velocity makes the three hinges position of projectile incursion into target. It is because of the surround restriction of penetration holes that new three hinges distributions arise and overlap each other sequentially. Therein axial crapy buckling occurs and it finally perforates the target plate like a blunt projectile.

Relatively lower impact velocities and weaker structural rigidity with larger length-diameter-ratio make the noses of projectiles III, IV, V and VI only partial incursion into targets. The targets can not completely constrain the motion of three-hinges along the enlarging hole. The subsequent evolutions of buckling after the rupture and fracture of the first three hinges are completely different from that of projectiles I and II. As shown in Fig.13 and Fig.14, the middle plastic hinge slides outwards along

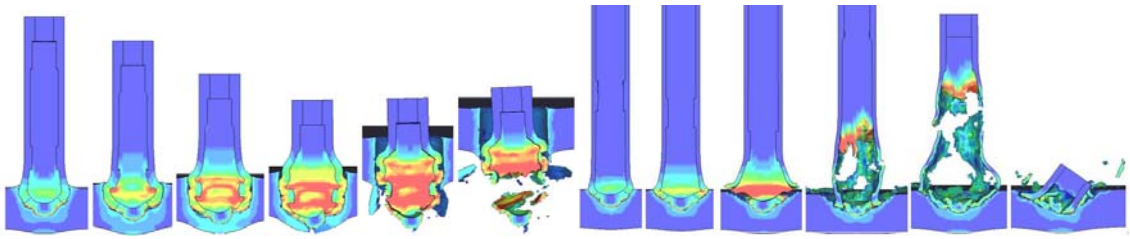

t=0.07, 0.1, 0.15, 0.25, 0.35, 0.45ms; t =0.06, 0.08, 0.12, 0.20, 0.25, 0.50ms

Figure 14. Simulations of axial crapy buckling of projectile II and axial evaginable tearing of projectile V

the surface of target and the last hinge moves backward to the tailend of projectile, which leads to the axial evaginable tearing of projectile shell. Especially, since the tearing velocity (equivalent to the velocity of travelling hinge) exceeds the impact velocity, projectile shell may tear and crash before it impinges on the target.

CONCLUSIONS

The present paper summarizes our recent studies on the failure and rapture of projectiles under penetration and perforation. Some new buckling and failure modes are identified by experimental study, and are further investigated by numerical simulations. Numerical results confirm these failure modes in the different scenarios and agree well with the experimental phenomena.

REFERENCES

[1] Yaziv D, Mayseless M and Reifen Y. Two Modes of Penetration Mechanisms of FSP Impact onto Steel Plates, *20th Int Symp Ballistics*, 847-854 (2002)
[2] Chen XW, Chen G, Zhang FJ. Three Failure Modes of A3 Steel Blunt Projectiles Impacting onto 45 Steel Plates. *Int J Impact Engng*, in review, 2006
[3] Chen XW, Zhang FJ, Liang B, et al. Three Modes of Penetration Mechanics of A3 steel Cylindrical Projectiles Impact onto 45 Steel Plates, *Explosions and Shock Waves* (in Chinese), **26(3)**:199-207(2006)
[4] Chen G, Chen XW, Chen ZF, et al. Simulations on the Penetrations of A3 steel Blunt Projectiles Impacting onto 45 Steel Plates, *Explosion and Shock Waves*(in Chinese), in press, 2006
[5] Darrigade A, Buzaud E. High performance concrete:A Numerical and experimental study, *18th Int Symp Ballistics*, 845-852(1999)
[6] Chen XW, Zhang FJ, Xu AM, et al., Buckling Analysis of Earth penetrating weapon and Equivalent Conditions of Targets. *Explosion and Shock Waves*(in Chinese), in press, 2006
[7] Qu M, Chen XW, Chen G. Numerical study on dynamic plastic buckling of EPW, *Explosion and Shock Waves* (in Chinese), in press, 2006